Interpretation of ^{31}P-NMR Coordination Shifts for Phosphane Ligands. Ab Initio ECP/DFT Study of Chemical Shift Tensors in $M(CO)_5L$ [M = Cr, Mo, W; L = PH_3, $P(CH_3)_3$, PF_3, PCl_3]☆

Martin Kaupp

Institut für Theoretische Chemie, Universität Stuttgart,
Pfaffenwaldring 55, D-70569 Stuttgart, Germany

Max-Planck-Institut für Festkörperforschung,
Heisenbergstraße 1, D-70569 Stuttgart, Germany
Telefax: (internat.) +49(0)711/689-1562; E-mail: kaupp@vsibm1.mpi-stuttgart.mpg.de

Received December 13, 1995

Key Words: Density-functional theory / ^{31}P-NMR chemical shift tensor / Quasirelativistic pseudopotential / Transition-metal phosphane complex

The ^{31}P chemical shift tensors of the transition-metal phosphane complexes $M(CO)_5PX_3$ (M = Cr, Mo, W; X = H, CH_3, F, Cl) were studied using a combination of density functional theory and ab initio effective-core potentials. The calculated isotropic shifts agree well with experimental results both for the free ligands and for the complexes, with the largest deviations occuring for the tungsten complexes. A breakdown of the computed phosphorus shielding tensors into contributions from localized molecular orbitals (LMOs) indicates that the positive coordination shift of PH_3 and $P(CH_3)_3$ is due to increased paramagnetic contributions from the phosphorus lone pair (P–M σ bonding) LMO to $\delta_\perp$. A similar increase of this contribution is found for PF_3 and PCl_3. However, for PCl_3 complexes these terms are overcompensated by a reduction in the paramagnetic contributions from the P–Cl bonds and by shielding contributions from metal-centered orbitals. This results in a negative overall coordiantion shift. A partial cancellation is found with $P(CH_3)_3$ and with PF_3. The changes in the ^{31}P-shift tensors of the same phosphane ligands upon protonation are qualitatively and quantitatively very different from the coordination shifts and do not provide good models for the latter.

Not long ago, Kutzelnigg et al. stated[1] that "a qualitative understanding of the rules that govern ^{31}P shifts has so far appeared to be a hopeless task". While a series of ab initio calculations by the Bochum group[1,2] and by others[3–5] on small to medium-sized phosphorus-containing molecules have improved this situation to some extent, the above statement unfortunately is still valid for the theoretical understanding of ^{31}P-NMR chemical shifts in transition-metal complexes[6,7]. This is due to the importance of electron correlation in systems containing transition metals[8]. Thus, the distributed-gauge-origin variants of the coupled Hartree-Fock (CHF) method, which have been very successful for the calculation and interpretation of NMR chemical shifts in "normal" main-group species[1,9], are not generally applicable to transition-metal compounds. The large cost in computational resources of recently developed post-CHF methods[10] (which account for electron correlation) has so far prevented their application to transition-metal complexes.

Recently, it has been shown that methods based on density functional theory (DFT) provide an attractive alternative to standard ab inito-correlated approaches to the calculation of NMR chemical shifts[11–21]. Due to the implicit inclusion of electron correlation with comparatively low computational effort, DFT methods are particularly suitable for transition-metal complexes. This also holds for the computation of NMR-chemical shift tensors, as demonstrated by our recent applications of the sum-over-states density-functional perturbation theory (SOS-DFPT) approach[11], e.g. to ^{13}C and ^{17}O shift tensors in carbonyl complexes[15,17] and clusters[20], to ^{17}O shifts in oxo complexes[16], and to ^{13}C shift tensors for interstitial carbides[21]. Scalar relativistic contributions may be included[15,16] in the calculations via quasirelativistic effective-core potentials (ECPs) for the heavy metals.

Here we report on the first application of this combined ECP/SOS-DFPT method to the calculation and interpretation of the ^{31}P-chemical shift tensors in transition-metal phosphane complexes. The trends of the ^{31}P coordination shifts (i.e. differences in shifts between coordinated and free ligands) for PX_3 ligands have been studied experimentally in great detail[6,7,22], but a conceptual understanding lags far behind. Thus, while e.g. the coordination shifts for organophosphane and PH_3 ligands correlate well with the shifts of the free ligands, this is not the case for, e.g., PCl_3, PBr_3, or PI_3. Moreover, some ligands exhibit positive coordination shifts, while others exhibit negative shifts. The origin of these trends is not, as of yet, understood[6,7,22]. Provided here is a detailed analysis of the ^{31}P shift tensors for the group-6 complexes $M(CO)_5L$ [M = Cr, Mo, W; L = PH_3, $P(CH_3)_3$, PF_3, PCl_3], the results of which are compared to shift changes upon protonation of the ligands. The

  0009–2940/96/0505–0535 $ 15.00+.25/0

computed carbonyl ^{13}C and ^{17}O shift tensors will be discussed elsewhere[23].

I. Computational Methods and Molecular Structures

As experimental structural parameters have only been available for some of the complexes, we have optimized the structures at the gradient-corrected DFT level with a modified version of the LCGTO-DFT program deMon[24] using the Becke-Perdew exchange-correlation functional[25]. These computations employed quasirelativistic energy-adjusted ECPs and (8s7p6d)/[6s5p3d] GTO valence basis sets for the metals[26,27] as well as ECPs and (4s4p1d)/[2s2p1d] valence bases for C, O, F, P, and Cl[28,29]. A (4s)/[2s] basis[30] was used for hydrogen. The transferability of ab initio ECPs into DFT applications has been studied in detail[31,32] and was found to be excellent for sufficiently small core sizes[31] (which holds for all of the ECPs employed here). Auxiliary basis sets for the fit of the exchange-correlation potential and of the charge density were of the size 3,3 for the metals, 3,2 for p-block elements, and 4,0 for hydrogen (*n,m* stands for *n* s functions and for *m* spd shells)[24]. A "FINE" integration grid[11,24] was used throughout in this study.

The optimized bond distances are listed in Table 1 together with available experimental data. The computed M–C, C–O, M–PH_3, and P–H distances agree with experiment to within 0.02–0.03 Å (apart from a few experimental values with large standard deviations) and all bond angles to within 1–3 deg. However, the P–F and M–P distances in the PF_3 complexes (and the P–F distances in free PF_3) as well as the P–C and M–P distances in the $P(CH_3)_3$ complexes are ca. 0.04 Å too long. Similarly, the P–Cl and M–PCl_3 distances obtained are ca. 0.08 Å too long at this computational level. This appears to be a problem of the gradient-corrected DFT approach rather than of the ECPs employed, as indicated by the data for PCl_3 given in Table 2 [similar but less dramatic differences between different functionals also hold for PF_3 and $P(CH_3)_3$]. As the deviations appear to be reasonably systematic, we decided to adjust the computed distances by corresponding amounts for use in the NMR-chemical shift calculations. Thus, the distances to phosphorus in PF_3 and $P(CH_3)_3$ complexes and in free PF_3 and $P(CH_3)_3$ have been reduced by 0.04 Å, those in the PCl_3 complexes and in PCl_3 by 0.08 Å. A similar correction could not be made for the protonated phosphanes due to the lack of experimental data. Thus, the structures of the PHX_3^+ cations were optimized at the MP2(full)/6-311G(D) level[33] with the Gaussian92/DFT program[34] (see Table 3).

All carbonyl complexes exhibit essentially octahedral metal coordination (with inter-ligand bond angles between 88 and 92°). The orientation of the PX_3 ligand in the optimized structures was generally such that one P–X bond was close to being eclipsed (with a dihedral angle of 12–13° for X = H, F, Cl, ca. 7° for X = CH_3) with one M–C_{cis} bond. This is consistent with the available experimental evidence[35].

The NMR chemical-shift calculations within the SOS-DFPT approach in its LOC1 approximation[11] used the same metal and chlorine ECPs and valence basis sets as the optimizations (see above), but IGLO-II all-electron basis sets[1] for H, C, O, F, and P. Auxiliary basis sets were of the sizes 3,4 for the metals, 3,3 for chlorine, 5,1 for hydrogen, 5,2 for C, O, and F, and 5,4 for P (cf. above). The exchange-correlation functional of Perdew and Wang (1991)[36] was employed, as in our previous ECP/SOS-DFPT calculations[15–18,20,21]. We used individual gauges for localized orbitals (IGLO)[1]. The Foster/Boys procedure[37] localized the phosphorus K shell separately, the phosphorus L shell together with the K shells of C, O, and F (they are in the same energy range), and the valence shell separately. A localization procedure which localized all orbitals together led systematically to 8–10 ppm lower absolute ^{31}P shieldings. However, the effect of the localization procedure on the shift differences between all of the species studied is generally below 2 ppm. We have preferred the separate localization, as the phosphorus L shell contributions to the shielding tensors obtained this way depend less on changes in the chemical environment (cf. section II.B.). All chemical-shift calculations were carried out with a modified version of the deMon-NMR program[11,24].

The ^{31}P relative chemical shifts are referenced to 85% H_3PO_4(aq) using the absolute shielding value of 328.4 ppm given by Jameson et al.[38]. The LMO analyses of the shielding tensors are based on computed absolute shieldings.

II. Results and Discussion

A. ^{31}P Chemical Shift Tensors

The ^{31}P shift tensors are summarized in Table 4 together with available experimental isotropic shifts [and tensor elements for PH_3, $P(CH_3)_3$ and PF_3, cf. footnote b]. Calculated and experimental isotropic shifts are also shown in Figure 1. The computed tensors for free PH_3 and PF_3 agree well with experiment[38], better than found for any of the ab initio methods [CHF, CHF(IGLO), CHF(LORG), SOLO, SOPPA] compared recently by Bouman and Hansen[5] (our results for PH_3 agree well with MP2 data due to Wolinski et al.[4d]). In particular, $\delta_{\|}$ for PF_3, which appears to be very difficult to compute[5,38], is only 33 ppm too low. The above-mentioned methods give values between 65 and 200 ppm too low, and electron-correlation corrections appear to be in the range of ca. 70 ppm[5].

The computed isotropic shift for $P(CH_3)_3$ agrees perfectly with experiment. Recent CHF(IGLO) results (with essentially the same basis sets as employed here) are ca. 40 ppm too low[1]. Our calculations suggest that $\delta_{\perp}$ for $P(CH_3)_3$ is somewhat more negative than $\delta_{\|}$, whereas the experimental data indicate the reverse[38] (cf. footnote b to Table 4). In view of the excellent agreement of the isotropic shift and of the computed tensors for PH_3 and PF_3 with experiment, it is not clear whether this is due to computational or to experimental errors. Possibly, the shielding anisotropy data (from liquid crystal solution) employed for the calculation of the experimental tensor[38] are not representative for the gas-phase species (if we use the anisotropy with opposite sign, we obtain reasonable agreement between computation

Table 1. Calculated (experimental) bond lengths [Å] and bond angles [deg]

	M-P	P-X	M-C_{trans}	M-C_{cis}	C-O_{trans}	C-O_{cis}	X-P-X
PH_3		1.443					92.4
		(1.420[a])					(93.3[a])
$Cr(CO)_5PH_3$	2.369	1.430	1.862	1.895	1.160	1.158	97.0
	(2.35[b])		(1.86[b])	(1.91[b])			
$Mo(CO)_5PH_3$	2.533	1.429	2.006	2.050	1.158	1.156	97.0
$W(CO)_5PH_3$	2.546	1.429	2.026	2.063	1.160	1.158	97.3
$P(CH_3)_3$		1.878					98.9
		(1.846[c])					(98.7[c])
$Cr(CO)_5P(CH_3)_3$	2.399	1.857	1.863	1.885	1.161	1.160	101.7
	(2.366[d])	(1.814[d])	(1.850[d])	(1.893[d])	(1.153[d])	(1.134[d])	(102.4[d])
$Mo(CO)_5P(CH_3)_3$	2.545	1.857	2.010	2.045	1.159	1.158	102.1
	(2.508[d])	(1.811[d])	(1.984[d])	(2.036[d])	(1.152[d])	(1.134[d])	(102.7[d])
$W(CO)_5P(CH_3)_3$	2.561	1.855	2.030	2.062	1.161	1.160	102.0
	(2.516[d])	(1.85[d])	(2.00[d])	(2.01[d])	(1.15[d])	(1.15[d])	(102.7[d])
PF_3		1.610					97.0
		(1.569[e])					(97.7[e])
$Cr(CO)_5PF_3$	2.235	1.601	1.883	1.895	1.154	1.154	97.2
$Mo(CO)_5PF_3$	2.407	1.600	2.030	2.058	1.153	1.152	97.4
	(2.369[f])	(1.557[f])			(av. 1.154[f])		(99.5[f])
$W(CO)_5PF_3$	2.405	1.598	2.048	2.070	1.155	1.154	97.5
PCl_3		2.119					101.0
		(2.04[g])					(100.4[g])
$Cr(CO)_5PCl_3$	2.277	2.103	1.877	1.896	1.156	1.154	99.9
	(2.245[d])	(2.025[d])	(1.900[d])	(1.905[d])	(1.141[d])	(1.130[d])	(99.6[d])
$Mo(CO)_5PCl_3$	2.457	2.106	2.021	2.059	1.155	1.152	99.5
$W(CO)_5PCl_3$	2.468	2.104	2.040	2.070	1.157	1.154	99.6
	(2.378[d])	(2.028[d])	(2.02[d])	(2.03[d])	(1.17[d])	(1.15[d])	(100.0[d])

[a] *Landolt-Börnstein, Zahlenwerte und Funktionen aus Naturwissenschaften und Technik* (Ed.: K. H. Hellwege), Springer, Berlin, **1976**. – [b] Estimated from data for $Cr(CO)_{6-n}(PH_3)_n$ (n = 2, 3), see L. J. Guggenberger, U. Klabunde, R. A. Schunn, *Inorg. Chem.* **1973**, *12*, 1143. – [c] P. S. Bryan, R. L. Kuczkowski, *J. Chem. Phys.* **1971**, *55*, 3049. – [d] Ref.[34]. – [e] Y. Morino, K. Kuchitsu, T. Moritani, *Inorg. Chem.* **1969**, *8*, 867. – [f] D. M. Bridges, G. C. Holywell, D. W. H. Rankin, J. M. Freeman, *J. Organomet. Chem.* **1971**, *32*, 87. – [g] P. Kisliuk, C. H. Townes, *J. Chem. Phys.* **1950**, *18*, 1109.

and theory[39]). Our isotropic shift for PCl_3 is too large by ca. 10 ppm, whereas CHF(IGLO) results are too low by ca. 30 ppm[1]. Apparently, electron correlation is moderate but far from negligible for these systems. We also estimate from preliminary calculations that spin-orbit coupling (which is neglected in the present work) may give shielding contributions of ca. 10–20 ppm for PCl_3 due to the presence of three chlorine substituents[40].

The computed isotropic shifts for $Cr(CO)_5PH_3$ and $Mo(CO)_5PH_3$ agree excellently with experiment, whereas the shift for $W(CO)_5PH_3$ is ca. 27 ppm too large. Thus, the positive coordination shift of PH_3 and the moderate de-

Table 2. P–Cl Distances [Å] in PCl_3 at various computational levels

functional	basis: ECP[a]	AE[b]
Hartree-Fock	2.063	2.052
MP2	2.080	2.057
BHandHLYP[c]	2.075	2.063
B3LYP[d]	2.104	2.093
BP86[e]	2.117	2.105

[a] ECPs and 2s2p1d valence bases[26,27]. – [b] All-electron 6-311(D) basis[33b]. – [c] Hybrid HF/DFT functional with 50% HF exchange, as proposed by Becke (A. D. Becke, *J. Phys. Chem.* **1993**, *98*, 1372) but as implemented in the G92/DFT program (ref.[32]) together with the LYP correlation functional (C. Lee, W. Yang, R. G. Parr, *Phys. Rev. B* **1988**, *37*, 785; B. Miehlich, A. Savin, H. Stoll, H. Preuss, *Chem. Phys. Lett.* **1989**, *157*, 200). – [d] Becke's three-parameter HF/DFT hybrid functional (A. D. Becke, *J. Chem. Phys.* **1993**, *98*, 5648), but in the G92/DFT implementation (cf. footnote c). – [e] Becke-Perdew functional (ref.[23]).

Table 3. MP2/6-311G*-Optimized structures of HPX_3^+. Optimized in C_{3v} symmetry. Distances in Å, angles in deg

X	P-H	P-X	H-P-X
H	1.393	1.393	109.5
CH_3	1.400	1.795	107.8
F	1.382	1.507	110.6
Cl	1.392	1.949	108.0

crease from M = Cr to M = Mo are given correctly, but the trend from M = Mo to M = W is wrong (Figure 1). We cannot say at present whether this is due to larger errors in the structure employed for the tungsten complex, to the neglect of spin-orbit coupling[15,17], or possibly to solvent effects. The coordination shift and the differences between different metals are due to changes in $\delta_\perp$, whereas $\delta_\parallel$ remains almost constant (Table 4). This is similar to the situation for the ^{13}C shifts in $M(CO)_6$ and is due to similar reasons[17] (see below)[*]. As a result, the shift anisotropy $\delta_\perp - \delta_\parallel$ changes sign from free to metal-bound PH_3 and decreases slightly down the metal triad [errors for $W(CO)_5PH_3$ have to be kept in mind]. In contrast to PF_3 and PCl_3, PH_3 exhibits a considerable increase in X–P–X bond angle (from ca. 92 to ca. 97°) upon coordination (Table 1). We have estimated the effect of this structural change on the shift tensor by performing a calculation on PH_3 with a P–H distance of 1.430 Å and an H–P–H angle

[*] **Note added in proof** (March 13, 1996): A recent solid-state NMR study of some phospholes and their metal complexes (K. Eichele, R. E. Wasylishen, J. M. Kessler, L. Solujić, J. H. Nelson, submitted to *Inorg. Chem.*; R. E. Wasylishen, personal communication) comes to the conclusion that the coordination shifts are dominated by $\delta_\perp$ whereas $\delta_\parallel$ changes little. This agrees with our results for PH_3 and $P(CH_3)_3$ complexes whereas the situation is more complicated for PF_3 and PCl_3 (Table 4).

Table 4. ^{31}P Shift tensors (ppm)[a]

	PH_3	$Cr(CO)_5PH_3$	$Mo(CO)_5PH_3$	$W(CO)_5PH_3$
$\delta_\perp$	-265.	-93.	-134.	-129.
$\delta_\parallel$	-218.	-221.	-225.	-226.
δ_{av} calctd.	-250.	-135.	-164.	-161.
δ_{av} exptl.[b]	-266.	-130.	-165.	-188.
$\delta_\perp-\delta_\parallel$	-47.	128.	91.	97.
	$P(CH_3)_3$	$Cr(CO)_5P(CH_3)_3$	$Mo(CO)_5P(CH_3)_3$	$W(CO)_5P(CH_3)_3$
$\delta_\perp$	-72.	32.	1.	0.
$\delta_\parallel$	-41.	-63.	-68.	-67.
δ_{av} calctd.	-61.	2.	-22.	-22.
δ_{av} exptl.[b]	-63.	7.	-17.	-36.
$\delta_\perp-\delta_\parallel$	-31.	95.	69.	67.
	PF_3	$Cr(CO)_5PF_3$	$Mo(CO)_5PF_3$	$W(CO)_5PF_3$
$\delta_\perp$	171.	314.	285.	272.
$\delta_\parallel$	-48.	-108.	-113.	-121.
δ_{av} calctd.	98.	173.	153.	141.
δ_{av} exptl.[b]	106.	174.[c]	147.	
$\delta_\perp-\delta_\parallel$	219.	422.	399.	394.
	PCl_3	$Cr(CO)_5PCl_3$	$Mo(CO)_5PCl_3$	$W(CO)_5PCl_3$
$\delta_\perp$	271.	319.	287.	265.
$\delta_\parallel$	138.	-17.	-28.	-49.
δ_{av} calctd.	227.	207.	182.	160.
δ_{av} exptl.	217.	187.		98.
$\delta_\perp-\delta_\parallel$	133.	336.	313.	314.

[a] Referenced to 80% H_3PO_4 via its absolute shielding of 328.4 ppm given in ref.[38]. – [b] Experimental values are gas-phase data for the free ligands (in the zero-pressure limit, cf. ref.[38]), and (unless noted otherwise) solution data for the complexes as summarized in ref.[6]. Ref.[38] gives the following shift tensor components for free ligands (in ppm): $\delta_\perp = -285$, $\delta_\parallel = -229$ (PH_3); $\delta_\perp = -61$, $\delta_\parallel = -68$ ($P(CH_3)_3$); $\delta_\perp = 166$, $\delta_\parallel = -15$ (PF_3). – [c] M. F. A. Dove, E. M. L. Jones, R. J. Clark, *Magn. Reson. Chem.* **1989**, *27*, 973.

Figure 1. Comparison of calculated and experimental isotropic ^{31}P shifts [in ppm vs. 80% H_3PO_4(aq)]. Dashed lines and open symbols correspond to calculated, solid or dotted lines and filled symbols refer to experimental data (cf. Table 4)

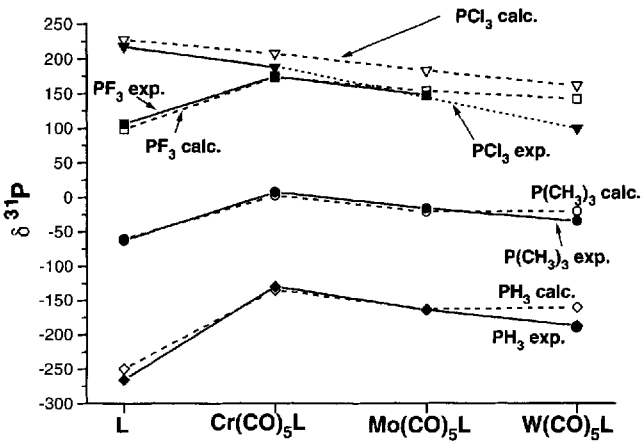

of 97°. The results are: $\delta_\perp = -243$ ppm, $\delta_\parallel = -201$ ppm, and $\delta_{iso} = -229$ ppm. Thus, the structural contributions to the positive coordination shift are ca. 20 ppm.

The calculated isotropic shifts of the $P(CH_3)_3$ complexes are also in good agreement with experiment (Table 4, Figure 1). Again, the coordination shift, which is considerably smaller than with PH_3, is reproduced well. The same holds for the decrease from Cr to Mo. The computed shift for the tungsten complex is again somewhat too large (by ca. 14 ppm). As for PH_3, the positive coordination shift is due to increased $\delta_\perp$[*]. However, $\delta_\parallel$ decreases by ca. 20–30 ppm and thus reduces the change in δ_{iso}. The same change in sign of the shift anisotropy is found upon coordination as for PH_3.

Excellent agreement with the experimental isotropic shifts is also found for $Cr(CO)_5PF_3$ and $Mo(CO)_5PF_3$, and thus the positive coordination shift of PF_3 is also reproduced correctly. Judging from the experimentally observed trends for the other ligands, the shift decrease from $Mo(CO)_5PF_3$ to $W(CO)_5PF_3$ is again underestimated (Figure 1), but the direction should be correct. The coordination shift is again due to an increase in $\delta_\perp$, partially compensated by reduced $\delta_\parallel$. This reduction of $\delta_\parallel$ (ca. 60–70 ppm) is considerably more pronounced than for the trimethylphosphane ligand (see above). Both $\delta_\perp$ and $\delta_\parallel$ decrease somewhat from Cr to W. The increase in shift anisotropy upon complex formation is even larger than with PH_3 [but in contrast to PH_3 and $P(CH_3)_3$, the sign of the anisotropy is already positive for free PF_3 and PCl_3].

The computed shift for $Cr(CO)_5PCl_3$ also agrees reasonably well with experiment (20 ppm too large), and thus the negative coordination shift of PCl_3 is also reproduced correctly. The decrease from Cr to W appears to be too small, and thus the error is signficant ($\delta_{iso}^{calc.}$ is 60 ppm too large) for $W(CO)_5PCl_3$ (Figure 1, Table 4). In contrast to PH_3, $P(CH_3)_3$ or PF_3, $\delta_\perp$ either increases much less or increases slightly upon complex formation, and there is a strikingly large decrease of $\delta_\parallel$ (by ca. 150–190 ppm). Thus, obviously the various contributions to the tensor elements must behave quite differently for PCl_3 than for the three other phosphane ligands (cf. below). The decrease of both $\delta_\perp$ and $\delta_\parallel$ from Cr to W is similar as for the PH_3, $P(CH_3)_3$, and PF_3 complexes. The increase in the shift anisotropy upon complex formation is very similar for PF_3 and PCl_3.

B. LMO Analysis of the ^{31}P Shielding Tensors

To obtain more insight into the reasons for the above trends, we have broken-down the absolute shielding tensors of the free ligands and of the complexes into contributions from the individual localized orbitals (LMOs) employed in the IGLO procedure[1]. Results for each ligand and its chromium complex are given in Tables 5–8. The results of the breakdown for free PH_3 and PF_3 are qualitatively similar to but quantitatively different from those obtained at the CHF(IGLO) level by Kutzelnigg et al.[1]. In particular, our phosphorus L shell contributions are considerably more positive and more invariant to changes in the chemical environment, whereas the P–X bond contributions (and the phosphorus lone-pair contribution for PH_3) are more negative and more variable. This is mainly due to our slightly different localization scheme (cf. computational details section). However, neither the overall chemical shifts nor the results of the qualitative interpretation are affected much by the localization procedure. One should keep these inherent ambiguities of an LMO separation in mind and refrain from overinterpretation of the results. While the phosphorus K shell contribution is constant at 516.3 ppm for all species considered, the L shell contributions vary over a range of ca. 40 ppm and are not completely isotropic. However, compared to changes in other contributions, these variations are minor, and we will not consider them in the following.

Table 5. LMO Analysis of phosphorus shielding tensors (ppm) for free and metal-bound PH_3[a]

LMO	PH_3			$Cr(CO)_5PH_3$		
	$\sigma_\perp$	$\sigma_\parallel$	σ_{av}	$\sigma_\perp$	$\sigma_\parallel$	σ_{av}
K shell(P)	516.3	516.3	516.3	516.3	516.3	516.3
L shell(P)	332.9	359.2	341.6	327.5	349.7	335.2
3xBd(P-H)	-120.5	-347.1	-196.1	-110.1	-361.7	-194.0
LP(P)/Bd(P-M)	-135.6	19.0	-83.9	-271.4	15.3	-175.8
ΣAO(M)				-37.9	26.2	-16.6
Σ[b]	593.2	547.4	577.9	425.0	545.8	465.1
Total:[c]	593.2	547.3	577.9	421.5	549.6	464.2

[a] Our notation is: Bd = bonding LMO, LP = lone-pair LMO, ΣAO(M) = sum of metal-centered LMO contributions. – [b] Sum of listed contributions. – [c] Sum of all contributions.

For free PH_3, the P–H bond contributions are deshielding, particularly for $\sigma_\parallel$ (Table 5). The phosphorus lone-pair contribution is deshielding for $\sigma_\perp$ but slightly shielding for $\sigma_\parallel$ (this is similar to the carbon or oxygen lone-pair contributions in free CO[1,17]). Upon coordination, the P–H bond contribution remains almost constant, but the contribution from the phosphorus lone-pair LMO (now being a P–M bonding orbital in the complex) to $\sigma_\perp$ becomes considerably more deshielding. A small additional deshielding contribution to $\sigma_\perp$ comes from metal-centered d and (n-1)p orbitals, similar to what is found for the ^{13}C shielding tensors in the hexacarbonyl complexes[17]. Neverthelcss, the bulk of the positive coordination shift for PH_3 is due to changes in only one LMO, the phosphorus lone-pair, which is transformed to a P–M bond upon coordination. This situation differs somewhat from the ^{13}C coordination shifts of carbonyl ligands[17] or of the other phosphane ligands discussed below, where several LMO contributions change. The coordination shifts of PH_3 may thus be rationalized somewhat easier than those of the other ligands.

The deshielding contributions from P–C bonds (to $\sigma_\perp$ and $\sigma_\parallel$) and phosphorus lone-pair (to $\sigma_\perp$) for free $P(CH_3)_3$ (Table 6) are larger than the corresponding P–H bond and

[*] See footnote on p. 538.

lone-pair contributions for PH_3 (Table 5), and they are augmented slightly by deshielding C–H bond contributions. As for PH_3, the coordination shift is dominated by the more deshielded $\sigma_\perp$ contribution from the phosphorus lone-pair (P–M bond) LMO. However, the change is only ca. 60 ppm for σ_{iso}, compared to ca. 90 ppm with PH_3, and the P–C bond and C–H bond contributions become slightly more shielding. Therefore, the overall deshielding coordination shift is smaller than for PH_3.

The deshielding contributions to $\sigma(^{31}P)$ in free PF_3 are also due to the P–X bonds and to the phosphorus lone-pair (Table 7). Both sets of LMOs are much more deshielding than for PH_3 and also more than for $P(CH_3)_3$ (cf. Tables 5, 6). Complex formation increases the deshielding contributions from the phosphorus lone-pair (now P–M bonding) LMO by almost the same amount as for PH_3, and the moderate additional deshielding due to metal-centered orbitals is very slightly larger than for PH_3 or $P(CH_3)_3$. However, the contributions from the P–F bonds decrease by ca. 30 ppm, and the fluorine lone-pair contributions become somewhat more shielding. As a result of this partial compensation, the overall positive coordination shift for PF_3 is ca. 40 ppm smaller than for PH_3, but still somewhat larger than for $P(CH_3)_3$.

Table 6. LMO Analysis of phosphorus shielding tensors (ppm) for free and metal-bound $P(CH_3)_3$. Cf. footnotes to Table 5.

LMO	$P(CH_3)_3$			$Cr(CO)_5P(CH_3)_3$		
	$\sigma_\perp$	$\sigma_\parallel$	σ_{av}	$\sigma_\perp$	$\sigma_\parallel$	σ_{av}
K shell(P)	516.3	516.3	516.3	516.3	516.3	516.3
L shell(P)	332.2	355.7	340.0	329.4	346.0	334.8
3xBd(P-C)	-216.6	-488.8	-307.4	-204.8	-484.4	-298.0
LP(P)/Bd(P-M)	-217.6	18.2	-139.0	-303.7	14.0	-197.8
ΣBd(C-H)	-13.0	-32.2	-19.8	1.1	-25.7	-8.2
ΣAO(M)				-38.6	23.9	-17.7
Σ[b]	401.3	369.2	390.1	299.6	390.1	329.4
Total:[c]	400.7	369.4	390.2	297.3	392.0	328.9

Table 7. LMO Analysis of phosphorus shielding tensors (ppm) for free and metal-bound PF_3. Cf. footnotes to Table 5

LMO	PF_3			$Cr(CO)_5PF_3$		
	$\sigma_\perp$	$\sigma_\parallel$	σ_{av}	$\sigma_\perp$	$\sigma_\parallel$	σ_{av}
K shell(P)	516.3	516.3	516.3	516.3	516.3	516.3
L shell(P)	362.3	397.2	374.0	361.3	393.2	371.9
3xBd(P-F)	-390.5	-520.0	-433.7	-355.0	-493.7	-400.5
LP(P)/Bd(P-M)	-352.9	20.1	-228.6	-506.0	16.7	-331.8
ΣLP(F)	23.0	-37.1	1.9	45.8	-24.3	22.5
ΣAO(M)				-48.0	28.2	-23.5
Σ	158.2	376.5	230.9	14.4	436.4	154.9
Total:	158.0	376.6	231.0	15.1	436.6	155.6

The P–Cl bonding LMOs in PCl_3 are even more deshielding than the P–F bonds in PF_3, whereas the phosphorus lone-pair is slightly less deshielding (Table 8). The chlorine lone-pairs make a significantly deshielding contribution in contrast to the fluorine lone-pairs in PF_3. Upon coordination, the deshielding phosphorus lone-pair (P–M bonding) contribution to $\sigma_\perp$ increases even more than for PH_3 and PF_3. However, the P–Cl bonds become much less deshielding (this holds for both $\sigma_\perp$ and $\sigma_\parallel$), the metal-centered LMOs are distinctly shielding, and the chlorine lone-pairs become slightly less deshielding. These contributions overcompensate the change in the phosphorus lone-pair contribution and result in an overall negative coordination shift for PCl_3. The large shielding contributions (mainly to $\sigma_\parallel$) from the "metal-centered" orbitals in the PCl_3 complexes (Table 8) contrast to corresponding deshielding effects found for the other three ligands (cf. Tables 5–7). The very large contributions from metal-centered LMOs may also partly account for the relatively large errors in our calculated shift for $W(CO)_5PCl_3$, as spin-orbit splitting of the 5d and 5p orbitals should appreciably modify these interactions[17].

Table 8. LMO Analysis of phosphorus shielding tensors (ppm) for free and metal-bound PCl_3. Cf. footnotes to Table 5

LMO	PCl_3			$Cr(CO)_5PCl_3$		
	$\sigma_\perp$	$\sigma_\parallel$	σ_{av}	$\sigma_\perp$	$\sigma_\parallel$	σ_{av}
K shell(P)	516.3	516.3	516.3	516.3	516.3	516.3
L shell(P)	351.9	380.3	361.3	343.4	370.5	352.6
3xBd(P-Cl)	-459.4	-634.8	-518.0	-358.3	-559.5	-425.4
LP(P)/Bd(P-M)	-304.1	20.7	-195.9	-468.5	17.0	-306.7
ΣLP(Cl)	-46.0	-91.6	-61.5	-32.2	-102.4	-50.2
ΣAO(M)				2.3	106.8	37.2
Σ	58.6	190.9	102.2	4.7	348.7	123.8
Total:	58.2	190.7	102.3	6.1	345.7	121.6

The considerably increased shift anisotropy values upon coordination are due to more deshielded $\sigma_\perp$ for PH_3, due to both more deshielded $\sigma_\perp$ and more shielded $\sigma_\parallel$ for PF_3 and $P(CH_3)_3$, and largely due to more shielded $\sigma_\parallel$ for PCl_3. These differences reflect mainly the relative importance of P–X bonding and phosphorus lone-pair LMO contributions (and of metal-centered LMO contributions as well) for these systems. The observed increase in shielding when going from Cr to Mo to W is dominated by reduced deshielding contributions form the P–M bonding LMO for the PH_3, $P(CH_3)_3$, and PF_3 complexes. This parallels our results for the ^{13}C shielding in the hexacarbonyl complexes, where the C–M bonding LMO is responsible for the same "triad effect"[17]. Matters are more complicated for the PCl_3 complexes, where P–Cl bonding LMOs become more deshielding from Cr to Mo whereas the metal-centered LMOs (and the P–M bond) become more shielding.

C. Analysis of ^{31}P Shielding Tensors in Terms of Canonical MOs

As calculations at the same basis-set level, but with a common gauge origin at the phosphorus nucleus, give results in reasonable agreement with the IGLO-based ones (deviations are typically in the 20-ppm range) and reproduce the important trends as well, it is also possible to carry out an analysis in terms of canonical orbitals. This allows the connection to the known MO diagrams of the ligands to be made (a similar analysis for free PF_3 has previously been given at the CHF level[3]).

Valence MO schemes for the ligands[41] are shown in Figure 2. The HOMO has in all four cases mainly phosphorus nonbonding character and is related to the lone-pair LMO discussed above. For PH_3 (Figure 2a), the next lower MOs (2e, $4a_1$) have P–H bonding character, whereas halogen-centered nonbonding MOs ($1a_2$, 6e, 5e) are inserted above the P–X bonding levels ($7a_1$, 4e) for PF_3 and PCl_3 (Figure 2b, c). Indeed, as shown in Table 9, the P–X bonding MOs (2e for PH_3, $7a_1$, 4e for the other ligands) and the P nonbonding MOs ($5a_1$ or $8a_1$, respectively) account for the major deshielding contributions to the ^{31}P shielding tensors in the free ligands (the phosphorus K shell contributions are 516.3 ppm, identical to the LMO analysis, the L shell contributions are ca. 388 ppm). Their relative importance does of course not exactly reflect the LMO results, as each canonical MO is related to several LMOs and vice versa.

Compared to PH_3, the gap between the most important occupied and empty levels in PF_3 is larger (cf. orbital energies in Figure 2b, a). Therefore, an explanation for the larger ^{31}P shift in PF_3 via the $(\Delta E)^{-1}$ factor of the Ramsey model[42] [or of individual $(\Delta E)^{-1}$ factors in the present sum-over-states ansatz] is unlikely. As the angular-momentum factors should also be smaller for PF_3[43], the larger paramagnetic contributions are probably best described as due to larger r^{-3} factors with the more electronegative fluorine substituents. PCl_3 exhibits still larger paramagnetic contributions than PF_3, in spite of presumably smaller r^{-3} factors. The much smaller gap between occupied and virtual levels [and thus larger $(\Delta E)^{-1}$ factors] is the most probable cause (cf. Figures 1c, b). With X = CH_3, the gap between occupied and virtual MOs is smaller than with X = H (Figure 2d), and in particular there is a large set of low-lying virtual MOs. This is probably the reason for the larger ^{31}P shift of $P(CH_3)_3$ compared to PH_3. The number of occupied MOs contributing to the shielding tensor for free $P(CH_3)_3$ is also larger (besides large contributions from the $8a_1$ and 6e MOs, the $7a_1$, 4e, and 5e MOs are also signifi-

Figure 2. Frontier MO diagrams based on the KS MOs used for the chemical shift calculations (cf. computational details section). a) PH_3. b) PF_3. c) PCl_3. d) $P(CH_3)_3$

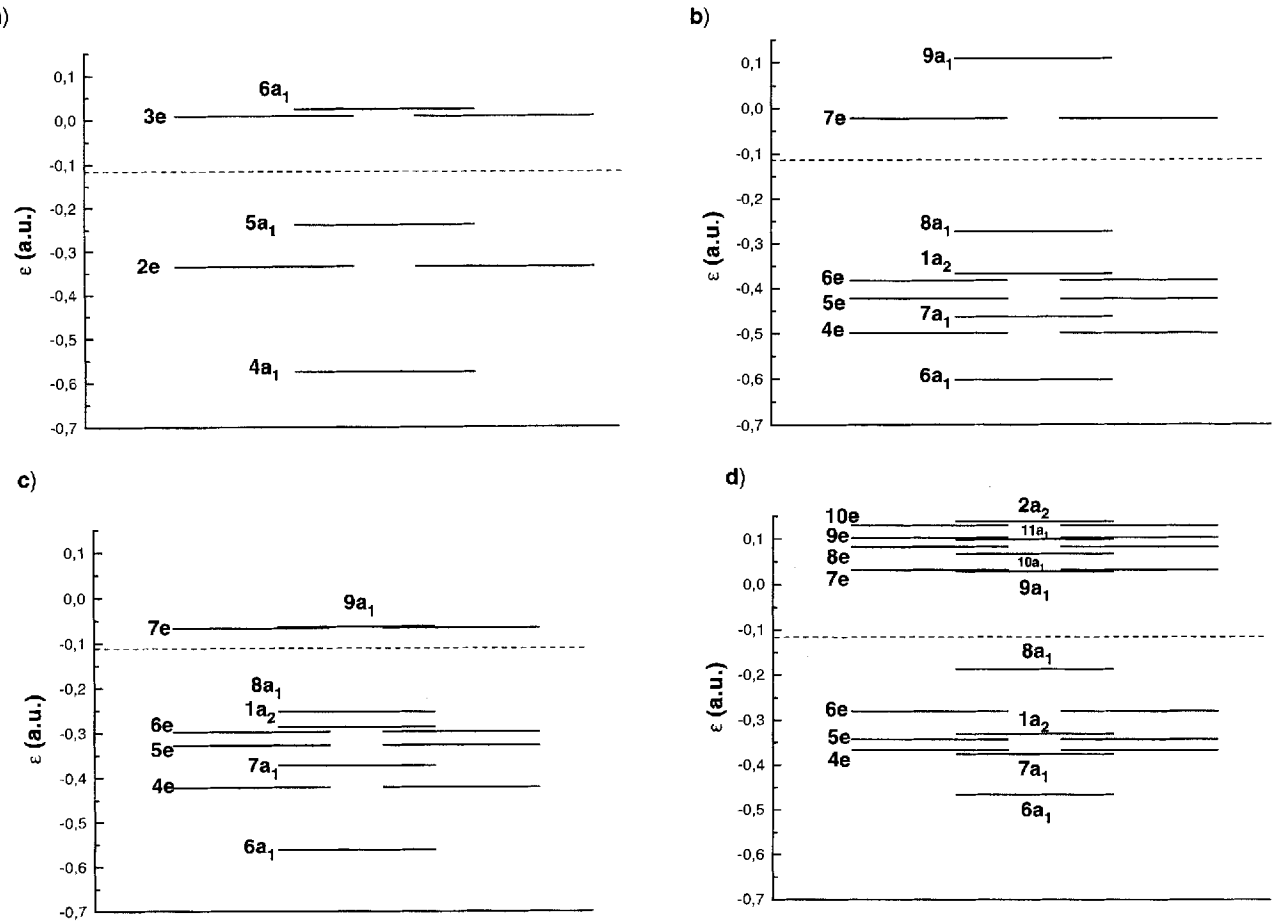

cantly involved) than for PF_3 and PCl_3. In the complex too many orbitals contribute, and the MO breakdown ceases to be useful. We have thus omitted the canonical MO analysis for $P(CH_3)_3$.

Comparison between the free ligands and their chromium complexes (Table 9, symmetry labels refer to the free-ligand origin of a given MO) indicates that for PH_3 all major valence MOs become more deshielding upon coordination. For PF_3, the "$8a_1$" MO becomes slightly more shielding and the others considerably more deshielding. Finally, for PCl_3 the "4e" and "$8a_1$" MOs become more shielding (this indicates, e.g., that the "$8a_1$" MO shares contributions from both the P–X bonding and the P lone-pair type LMOs discussed in the preceding section), and only the "$7a_1$" MO is somewhat more deshielding in the complex.

Table 9. Major deshielding canonical MO contributions to ^{31}P shielding tensors (ppm)[a]

MO	PH_3			$Cr(CO)_5PH_3$		
	$\sigma_\perp$	$\sigma_\parallel$	σ_{av}	$\sigma_\perp$	$\sigma_\parallel$	σ_{av}
"2e"	-38.9	-403.1	-160.3	-193.2	-247.0	-211.3
"$5a_1$"	-284.6	13.7	-185.1	-334.2	10.1	-219.4
Total:	590.5	536.1	572.4	440.0	552.1	477.4
MO	PF_3			$Cr(CO)_5PF_3$		
	$\sigma_\perp$	$\sigma_\parallel$	σ_{av}	$\sigma_\perp$	$\sigma_\parallel$	σ_{av}
"4e"	-148.3	-273.8	-140.7	-185.0	-440.7	-268.9
"$7a_1$"	-63.6	8.5	-39.5	-144.3	7.4	-93.7
"$8a_1$"	-503.4	10.7	-332.0	-440.8	7.3	-291.4
Total:	181.6	385.0	249.4	41.1	468.8	183.7
MO	PCl_3			$Cr(CO)_5PCl_3$		
	$\sigma_\perp$	$\sigma_\parallel$	σ_{av}	$\sigma_\perp$	$\sigma_\parallel$	σ_{av}
"4e"	-770.2	-225.0	-406.7	-545.8	-167.7	-193.7
"$7a_1$"	-175.9	8.3	-114.5	-202.7	3.5	-134.0
"$8a_1$"	-464.7	5.9	-307.8	-360.1	3.7	-238.8
Total:	56.5	186.9	100.0	362.5	23.4	136.4

[a] Obtained from calculations with common gauge origin at the phosphorus nucleus. MO symmetry labels are those appropriate for the free ligands (cf. Figure 1). The phosphorus K and L shell contributions are +516.3 and ca. +388 ppm, respectively. Only MO contributions to σ_{av} more deshielding than −30 ppm have been considered.

It is notable that essentially all of the major contributing occupied MOs are stabilized upon coordination (on the average by ca. 0.05 a.u.). Thus, the positive coordination shifts for PH_3, PF_3, or $P(CH_3)_3$ may not be attributed to reduced (ΔE^{-1}) factors in the sum-over-states expression for paramagnetic shielding via destabilization of occupied levels. More likely, the larger number of low-lying virtual levels and increased r^{-3} factors (population analyses clearly support net charge donation from the ligands to the metal fragments) account for the deshielding upon coordination. Further breakdown of the sum-over-states expression into contributions from individual electronic excitations shows that for the free ligands only the lowest-lying virtual orbitals are important for the shielding tensors. This changes dramatically upon complex formation. While the contributions from the most important occupied "ligand" MOs are still recognizable (Table 9) and augmented by metal-dominated MO contributions, the number of contributing low-lying virtual orbitals increases sharply (also cf. ref.[17]). This prohibits a detailed analysis of the computed trends in terms of just a few individual electronic excitations.

D. Comparison to ^{31}P Protonation Shifts

Several authors have drawn parallels between the ^{31}P shifts of phosphane ligands and the shift changes upon protonation of these phosphanes[6,45]. Thus, it is of interest to examine to what extent protonation shifts may serve as models for coordination shifts. Table 10 shows the computed shielding tensors for the protonated ligands and results of the corresponding LMO analyses. Compared to the experimental values of −16 and −87 ppm[44], the computed protonation shifts for PF_3 and PCl_3 of −78 and −140 ppm, respectively, are too negative. The protonation shift for PH_3 is calculated to be +98 ppm [in good agreement with CHF(IGLO) results[1]] compared to an experimental value of +139 ppm[45]. The best agreement between calculation and experiment (+38 vs. +59 ppm[45]) is found for the protonation shift of $P(CH_3)_3$. Thus, the computed shifts for the protonated species are generally lower than experiment. However, the experimental values have been obtained in solution, and for these ionic species the gas-liquid shift may be large.

It is immediately obvious from a comparison of the data in Table 10 to those of Tables 5–8, that the changes upon protonation and upon coordination to a $M(CO)_5$ fragment are very different. While the protonation shifts of PH_3 and $P(CH_3)_3$ are positive, those of PF_3 and PCl_3 are both negative (for PF_3, the coordination shift is positive). More importantly, compared to the changes upon coordination (Tables 5–8), the tensor elements are affected differently. Thus, for PF_3 and PCl_3 protonation leads to more shielded $\sigma_\perp$ but less shielded $\sigma_\parallel$ (Table 10). For PH_3 and $P(CH_3)_3$, all components become more deshielded.

The LMO analysis (Table 10) indicates that protonation of the phosphorus "lone-pair" reduces the deshielding contributions from this LMO to $\sigma_\perp$, except for PH_4^+ [coordination to $M(CO)_5$ generally increases this contribution, cf. Tables 5–8]. The contributions from the P–X bonds behave very irregularly. They become more deshielding to $\sigma_\perp$ and more shielding to $\sigma_\parallel$ for PH_3, vice versa for PF_3 and PCl_3, and generally more deshielding for $P(CH_3)_3$. The halogen lone-pair LMOs also become more shielding. Thus, most LMO contributions change in the opposite direction upon protonation compared with binding to a transition-metal fragment. The structural changes (of both angles and bond lengths) upon protonation are more dramatic than

Table 10. LMO Analysis of ^{31}P shielding tensors (ppm) for protonated phosphanes. Cf. data for unprotonated ligands in Tables 5–8

LMO	PH_4^+	$PH(CH_3)_3^+$		
	σ_{av}	$\sigma_\perp$	$\sigma_\parallel$	σ_{av}
K shell(P)	516.3	516.3	516.3	516.3
L shell(P)	329.6	338.5	331.4	336.2
3xBd(P-X)	-280.6	-339.4	-526.3	-401.8
Bd(P-H)	-93.6	-143.3	9.8	-92.3
ΣBd(C-H)		2.8	-25.3	-5.6
Total:	471.6	374.8	305.7	351.8

LMO	PHF_3^+			$PHCl_3^+$		
	$\sigma_\perp$	$\sigma_\parallel$	σ_{av}	$\sigma_\perp$	$\sigma_\parallel$	σ_{av}
K shell(P)	516.3	516.3	516.3	516.3	516.3	516.3
L shell(P)	368.2	385.9	374.1	343.6	360.2	349.0
3xBd(P-X)	-371.7	-602.9	-449.3	-399.4	-705.3	-501.1
Bd(P-H)	-262.0	11.2	-170.9	-233.1	10.9	-151.9
ΣLP(X)	77.0	-10.9	47.7	66.7	-45.3	29.4
Total:	328.1	299.5	318.6	294.5	136.3	241.8

for the coordination to an $M(CO)_5$ fragment. This holds particularly for PH_3, where the H–P–H angle of 92° contrasts to 109.5° in tetrahedral PH_4^+, and also for $P(CH_3)_3$ (cf. Tables 1, 3). Therefore, the structural effects on the protonation shifts are also more pronounced. A calculation on PH_4^+ with the optimized P–H distance of 1.393 Å but with a C_{3v} arrangement (the smallest H–P–H angles being 92°) gives $\sigma_\perp$ = 511 ppm, $\sigma_\parallel$ = 555 ppm, and σ_{iso} = 526 ppm. Hence, the bond-angle changes contribute ca. +50 ppm to the protonation shift of +100 ppm. Somewhat less pronounced structural effects pertain to PF_3 and PCl_3.

III. Conclusions

The results of the present study confirm that ^{31}P coordination shifts of substituted phosphane ligands in transition-metal complexes are not easily interpretable. The detailed electronic structure of the ligand has to be taken into account, and a considerable number of orbitals may be involved in changes of the shift tensors. Nevertheless, some useful generalizations have been obtained: When, within the framework of an LMO analysis, the coordination shift is dominated by the contributions from the phosphorus lone-pair/P–M bonding orbital, as for PH_3 and $P(CH_3)_3$ (and probably for trialkyl- or triarylphosphanes in general), the coordination shift is positive, due to increased deshielding of this LMO (via $\sigma_\perp$). Contributions from the P–X bonds become increasingly more shielding upon coordination along the series $PH_3 < P(CH_3)_3 < PF_3 < PCl_3$. For trichlorophosphane these changes, augmented by metal-centered LMO contributions, finally overcompensate the changes in the phosphorus lone-pair contributions, and the coordination shift is negative. Metal-centered LMO contributions are shielding for PCl_3 complexes but predominantly deshielding for the other ligands. This observation will require further investigation. The shift anisotropy generally increases considerably upon coordination, and it decreases slightly from Cr to Mo to W. The decrease of the isotropic shift along the same series is due to a corresponding decrease in the deshielding contributions from the P–M bonding LMO for the PH_3, $P(CH_3)_3$, and PF_3 complexes (in analogy to results for the ^{13}C shifts for CO ligands[17]). A larger number of LMO contributions change for the PCl_3 complexes.

Protonation shifts are poor analogues to the coordination shifts. The parallel and perpendicular shift tensor elements are affected in an almost consistently opposite way by protonation compared with the coordination to a transition-metal fragment. The structural changes induced by protonation are also much larger than those due to the complex formation. It is thus gratifying that the combined ECP/SOS-DFPT approach allows the direct and accurate calculation of the ^{31}P ligand chemical shifts in transition-metal complexes. The somewhat larger deviations from experiment for the tungsten complexes will have to be examined to improve the calculations. Possibly, spin-orbit coupling has to be included for the 5d metal, and work along these lines is in progress[40]. In view of the considerable importance of ^{31}P-NMR spectroscopy in transition-metal chemistry[6,7], the availability of a reliable tool for the calculation of phosphorus chemical shifts is encouraging. Apart from providing a better understanding of the rules that determine the chemical shifts, these new methods are also expected to be helpful in solving structural or mechanistic problems.

I am grateful to Dr. *V. G. Malkin* and *O. L. Malkina* (Bratislava) for stimulating discussions. I also thank the *Deutsche Forschungsgemeinschaft* for a Habilitationsstipendium and Prof. *H. G. von Schnering* (Max-Planck-Institut Stuttgart) and Prof. *H.-J. Werner* (Universität Stuttgart) for their support and for providing computational resources.

☆ Dedicated to Professor *Hans Georg von Schnering* on the occasion of his 65th birthday.

[1] W. Kutzelnigg, U. Fleischer, M. Schindler in *NMR-Basic Principles and Progress*, Springer Verlag, Heidelberg, **1990**, vol. 23, p. 165.
[2] U. Fleischer, M. Schindler, W. Kutzelnigg, *J. Chem. Phys.* **1987**, *86*, 6337.
[3] J. A. Tossell, P. Lazzeretti, *J. Chem. Phys.* **1987**, *86*, 4066.
[4] [4a] D. B. Chesnut, B. E. Rusiloski, *Chem. Phys.* **1991**, *157*, 105. – [4b] D. B. Chesnut, L. D. Quin, K. D. Moore, *J. Am. Chem. Soc.* **1993**, *115*, 11984. – [4c] M. Häser, U. Schneider, R. Ahlrichs, *J. Am. Chem. Soc.* **1992**, *114*, 9551. – [4d] K. Wolinski, C.-L. Hsu, J. F. Hinton, P. Pulay, *J. Chem. Phys.* **1993**, *99*, 7819.
[5] T. D. Bouman, A. E. Hansen, *Chem. Phys. Lett.* **1990**, *175*, 292.
[6] K. R. Dixon in *Multinuclear NMR* (Ed.: J. Mason), Plenum Press, New York, **1987**, pp. 369ff.
[7] *^{31}P and ^{13}C NMR of Transition Metal Phosphine Complexes* (Eds.: P. S. Pregosin, R. W. Kunz), Springer, Berlin, **1979**.
[8] *The Challenge of f- and d-Orbitals* (Eds.: D. R. Salahub, M. Zerner), The American Chemical Society, Washington, D. C., **1989**.

[9] For a recent overview, cf.: *Nuclear Magnetic Shieldings and Molecular Structure* (Ed.: J. A. Tossel), Kluwer Academic Publishers, Dordrecht, **1993**.
[10] Cf., e.g.: W. Kutzelnigg, C. v. Wüllen, U. Fleischer, R. Franke, T. v. Mourik in ref.[9], p. 141; S. P. A. Sauer, I. Paidarova, J. Oddershede, *Mol. Phys.* **1994**, *81*, 87; J. Gauss, *J. Chem. Phys.* **1993**, *99*, 3629; K. Ruud, T. Helgaker, R. Kobayashi, P. Jorgensen, K. L. Bak, H. J. Aa. Jensen, *ibid.* **1994**, *100*, 8178; H. Fukui, T. Baba, H. Matsuda, K. Miura, *ibid.* **1994**, *100*, 6608; J. Gauss, *Chem. Phys. Lett.* **1994**, *229*, 198; J. Gauss, J. F. Stanton, *J. Chem. Phys.* **1995**, *102*, 251; M. Bühl, J. Gauss, J. F. Stanton, *Chem. Phys. Lett.* **1995**, *241*, 248; J. Gauss, J. F. Stanton, *J. Chem. Phys.* **1995**, *103*, 3561; J. Gauss, J. F. Stanton, *J. Chem. Phys.* **1996**, *104*, 2574; C. v. Wüllen, W. Kutzelnigg, *J. Chem. Phys.* **1996**, *104*, 2330.
[11] [11a] V. G. Malkin, O. L. Malkina, M. E. Casida, D. R. Salahub, *J. Am. Chem. Soc.* **1994**, *116*, 5898. – [11b] V. G. Malkin, O. L. Malkina, L. A. Eriksson, D. R. Salahub in *Theoretical and Computational Chemistry*, vol. 2 (Eds.: P. Politzer, J. M. Seminario), Elsevier, Amsterdam, **1995**.
[12] V. G. Malkin, O. L. Malkina, D. R. Salahub, *Chem. Phys. Lett.* **1993**, *204*, 80.
[13] V. G. Malkin, O. L. Malkina, D. R. Salahub, *Chem. Phys. Lett.* **1993**, *204*, 87.
[14] For more applications of the SOS-DFPT approach with main-group species, cf.: T. B. Woolf, V. G. Malkin, O. L. Malkina, D. R. Salahub, B. Roux, *Chem. Phys. Lett.* **1995**, *239*, 186; V. G. Malkin, O. L. Malkina, D. R. Salahub, *J. Am. Chem. Soc.* **1995**, *117*, 3294; V. G. Malkin, O. L. Malkina, G. Steinebrunner, H. Huber, *Chem. Eur. J.*, in press.
[15] M. Kaupp, V. G. Malkin, O. L. Malkina, D. R. Salahub, *Chem. Phys. Lett.* **1995**, *235*, 382.
[16] M. Kaupp, V. G. Malkin, O. L. Malkina, D. R. Salahub, *J. Am. Chem. Soc.* **1995**, *117*, 1851; **1995**, *117*, 8492.
[17] M. Kaupp, V. G. Malkin, O. L. Malkina, D. R. Salahub, *Chem. Eur. J.* **1996**, *2*, 24.
[18] M. Kaupp, *Chem. Eur. J.* **1996**, *2*, 194.
[19] G. Schreckenbach, T. Ziegler, *J. Phys. Chem.* **1995**, *99*, 606.
[20] M. Kaupp, *Chem. Ber.* **1996**, *129*, 527–533; preceding paper.
[21] M. Kaupp, submitted (interstitial carbides).
[22] Papers dealing with experimental work on ^{31}P shifts in phosphane complexes and with their interpretation are already too numerous to be quoted here in detail. Some papers will be mentioned during the discussion. For many others, the reader is referred to the bibliographies in refs.[6,7].
[23] M. Kaupp, in preparation.
[24] D. R. Salahub, R. Fournier, P. Mlynarski, I. Papai, A. St-Amant, J. Ushio in *Density Functional Methods in Chemistry* (Eds.: J. K. Labanowski, J. W. Andzelm), Springer, New York, **1991**, p. 77; A. St-Amant, D. R. Salahub, *Chem. Phys. Lett.* **1990**, *169*, 387; A. St-Amant, Thesis, Université de Montréal, **1992**.
[25] A. D. Becke, *Phys. Rev. A* **1988**, *38*, 3098; J. P. Perdew, *Phys. Rev. B* **1986**, *33*, 8822.
[26] M. Dolg, U. Wedig, H. Stoll, H. Preuss, *J. Chem. Phys.* **1987**, *86*, 866.
[27] D. Andrae, U. Häußermann, M. Dolg, H. Stoll, H. Preuss, *Theor. Chim. Acta* **1990**, *77*, 123.
[28] A. Bergner, M. Dolg, W. Küchle, H. Stoll, H. Preuss, *Mol. Phys.* **1993**, *80*, 1431.
[29] The halogen valence bases are from: M. Kaupp, P. v. R. Schleyer, H. Stoll, H. Preuss, *J. Am. Chem. Soc.* **1991**, *113*, 6012.
[30] N. Godbout, D. R. Salahub, J. Andzelm, E. Wimmer, *Can. J. Chem.* **1992**, *70*, 560.
[31] M. Kaupp, H.-J. Flad, A. Köster, H. Stoll, D. R. Salahub, in preparation.
[32] [32a] C. van Wüllen, *Int. J. Quant. Chem.*, in press. – [32b] T. V. Russo, R. L. Martin, P. J. Hay, *J. Phys. Chem.* **1995**, *99*, 17085.
[33] [33a] R. Krishnan, J. S. Binkley, R. Seeger, J. A. Pople, *J. Chem. Phys.* **1980**, *72*, 650. – [33b] A. D. McLean, G. S. Chandler, *J. Chem. Phys.* **1980**, *72*, 5639.
[34] *Gaussian 92/DFT*, Revision G, M. J. Frisch, G. W. Trucks, M. Head-Gordon, P. M. W. Gill, M. W. Wong, J. B. Foresman, B. G. Johnson, H. B. Schlegel, M. A. Robb, E. S. Replogle, R. Gomperts, J. L. Andres, K. Raghavachari, J. S. Binkley, C. Gonzalez, R. L. Martin, D. I. Fox, D. J. DeFrees, J. Baker, J. P. Stewart, J. A. Pople, Gaussian, Inc., Pittsburgh PA, **1992**.
[35] M. S. Davies, M. J. Aroney, I. E. Buys, T. W. Hambley, J. E. Calvert, *Inorg. Chem.* **1995**, *34*, 330.
[36] J. P. Perdew, Y. Wang, *Phys. Rev. B* **1992**, *45*, 13244; J. P. Perdew in *Electronic Structure of Solids* (Eds.: P. Ziesche, H. Eischrig), Akademie Verlag, Berlin, **1991**; J. P. Perdew, J. A. Chevary, S. H. Vosko, K. A. Jackson, M. R. Pederson, D. J. Singh, C. Fiolhais, *Phys. Rev. B* **1992**, *46*, 6671.
[37] J. M. Foster, S. F. Boys, *Rev. Mod. Phys.* **1963**, *35*, 457.
[38] C. J. Jameson, A. de Dios, A. K. Jameson, *Chem. Phys. Lett.* **1990**, *167*, 575.
[39] CHF(GIAO) calculations with the same basis sets also give $\delta_\perp < \delta_\parallel$ for the ^{31}P shift tensor of $P(CH_3)_3$.
[40] V. G. Malkin, O. L. Malkina, M. Kaupp, unpublished results.
[41] For earlier DFT calculations on PH_3 and PF_3, cf.: S.-X. Xiao, W. C. Trogler, D. E. Ellis, Z. Berkovich-Yellin, *J. Am. Chem. Soc.* **1983**, *105*, 7033.
[42] N. F. Ramsey, *Phys. Rev.* **1950**, *77*, 567; **1950**, *78*, 567; **1951**, *83*, 540; **1952**, *86*, 243.
[43] Calculations on fluorine-substituted lead compounds (M. Kaupp, P. v. R. Schleyer, *J. Am. Chem. Soc.* **1993**, *115*, 1061) have shown that electronegative substituents like fluorine increase the hybridization defects (W. Kutzelnigg, *Angew. Chem.* **1984**, *96*, 262; *Angew. Chem. Int. Ed. Engl.* **1984**, *23*, 272) for the central p-block main-group atom. Thus, the p orbitals are more depleted than the s orbitals. This should reduce the angular-momentum factor of the Ramsey expression.
[44] L. J. Vande Griend, J. G. Verkade, *J. Am. Chem. Soc.* **1975**, *97*, 5958.
[45] E. Moser, E. O. Fischer, W. Bathelt, W. Gretner, L. Knauss, E. Louis, *J. Organomet. Chem.* **1969**, *19*, 377; G. A. Olah, C. W. McFarland, *J. Org. Chem.* **1969**, *34*, 1832.

[96027]